

# Rapid estimation of ground-shaking maps for seismic emergency management in the Campania Region of southern Italy

Vincenzo Convertito · Raffaella De Matteis · Luciana Cantore · Aldo Zollo · Giovanni Iannaccone · Mauro Caccavale

Received: 28 July 2008 / Accepted: 30 January 2009  
© Springer Science+Business Media B.V. 2009

**Abstract** Strong ground-shaking mapping soon after a moderate-to-large earthquake is crucial to recognize the areas that have suffered the largest damage and losses. These maps have a fundamental role for emergency services, loss estimation and planning of emergency actions by the Civil Protection Authorities. This is particularly important for areas with high seismic risk levels, such as the Campania-Lucania Region in southern Italy. Taking advantage of the Irpinia Seismic Network (ISNet), a recently installed dense and wide dynamic seismic network, we have developed a procedure for rapid estimation of ground-shaking maps after moderate-to-large earthquakes (GRSmap). This uses an optimal data gridding scheme designed to account for bi-dimensional features of strong ground-motion fields, such as directivity, radiation patterns and focal mechanisms, to which most damage can be correlated. The basis of the mapping technique is a triangulation procedure to locally correct predicted data at the triangle barycentres where their vertices correspond to seismic stations. The method has been tested off-line using a simulated  $M$  6.6 earthquake located at the centre of ISNet and applied to data of the 23 November 1980 Irpinia  $M$  6.9 earthquake recorded by a sparse network. This has highlighted its ability to predict peak ground-motion parameters of large magnitude earthquakes with respect to the attenuation relationships.

**Keywords** Ground-shaking maps · Triangulation scheme · Seismic source · Seismic network · Seismic hazard

---

V. Convertito (✉) · G. Iannaccone  
Istituto Nazionale di Geofisica e Vulcanologia, Osservatorio Vesuviano, Naples, Italy  
e-mail: convertito@ov.ingv.it

R. De Matteis  
Dipartimento di Studi Geologici ed Ambientali, Università degli Studi del Sannio, Benevento, Italy

L. Cantore · A. Zollo · M. Caccavale  
Dipartimento di Scienze Fisiche, Università degli Studi di Napoli "Federico II", Naples, Italy

## 1 Introduction

The Campania-Lucania Region in the southern Apennines is one of the highest seismic hazard areas in Italy (Cinti et al. 2004). It has experienced numerous disastrous seismic events, among which there were those of 1694, 1851, 1857 and 1930. The most recent event was the complex normal-faulting 23 November 1980  $M_S$  6.9 Irpinia earthquake, which resulted in about 3,000 victims and huge damage to the historical and civil heritage (Westaway and Jackson 1984; Bernard and Zollo 1989). The present-day seismicity in this area is characterized by low-to-moderate magnitude events that are mainly concentrated along the seismogenic structures on which the 23 November 1980 Irpinia earthquake originated. Along with the presence of densely populated cities and wide dissemination of industrial facilities, these considerations make Campania-Lucania, a region of high seismic risk.

With the aim of mitigating the potential impact of large or very frequent moderate earthquakes, an Earthquake Early Warning System (EWS) prototype is under development in the Campania-Lucania Region. The core of the EWS is the Irpinia Seismic Network (ISNet) (Fig. 1), which covers an area of approximately  $100 \text{ km} \times 70 \text{ km}$  along the southern Apennine chain, and is deployed around and over the active fault system that generated the 1980 Irpinia earthquake. ISNet is equipped with sensors that can record high-quality seismic signals from both small magnitude and strong earthquakes. Due to its high density (inter-station distance, 10 km), wide dynamic range, and advanced data-acquisition and data-transmission technologies, ISNet is devoted on the one hand to real-time estimations of earthquake locations and magnitudes and on the other hand to the rapid provision of information for the Regional Civil Protection Authorities relating to the impact of the detected earthquakes, by providing rapid maps of peak ground-motion-parameter distributions.

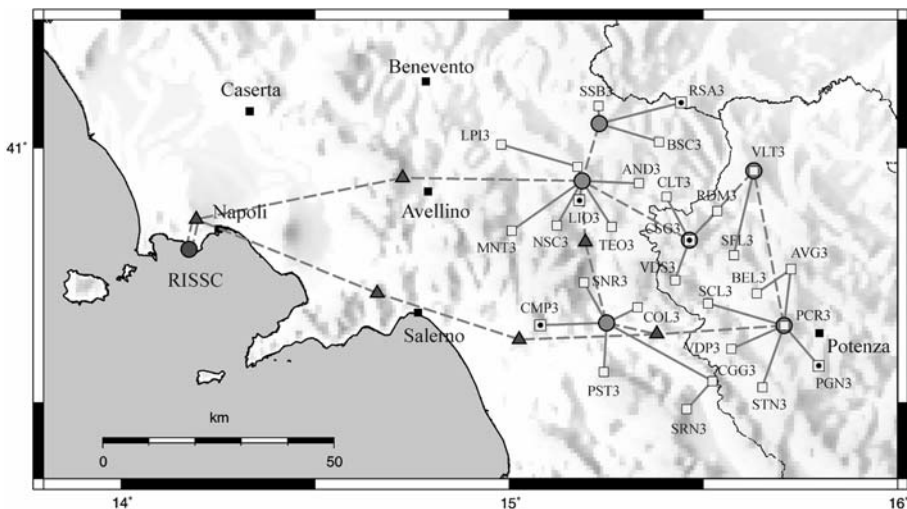


**Fig. 1** The Irpinia Seismic Network (ISNet) configuration. The LCC locations (grey circles) and the RISSC in Naples are also shown (from Weber et al. 2007). The lines refer to the different transmission techniques used to connect the stations, LCCs and the RISSC

The provision of this strong ground-shaking mapping soon after a moderate-to-large earthquake is crucial for the identification of the areas that could have suffered the greatest damage and losses. The usefulness of ground-shaking maps basically depends on their ability to reproduce the real pattern of damage and on the rapidity with which they are made available to the authorities in charge of managing rescue procedures. Apart from magnitude and location estimates, the reliability of ground-shaking maps is mainly related to the spatial density of the seismic network where the data are recorded and to the accuracy of the tools used to extrapolate the ground motion in areas not covered by the network. Generally, the maps are made by integrating automatically recorded data and predicted data at a set of virtual stations by means of averaging schemes that can assign different weights to recorded and predicted data. This idea was developed by Wald et al. (1999a), who introduced the ShakeMap<sup>®</sup> code for ground-shaking maps, which is now used worldwide.

The tool used to estimate ground-motion parameters depends on the time-scale of interest. For near-real-time applications, pre-existing empirical attenuation relationships are generally used (Wald et al. 1999a; Goltz 2003; Jean et al. 2006). On the other hand, theoretical approaches based on finite-fault models can be used to compute maps in post-event periods (Dreger and Kaverina 2000). Currently, real-time approaches have also been proposed to generate ground-shaking distributions that are updated as more data concerning magnitude, location and selected ground-motion parameters, such as peak ground acceleration (PGA) and peak ground velocity (PGV), become available. This is the case for the ElarmS methodology proposed by Allen (2007), which generates an 'AlertMap' using a radial attenuation relationship that is updated every second. However, when attenuation relationships are used to estimate ground motion, two main problems have to be considered. First, ground motion has to be estimated in the same region where the data used to retrieve the attenuation model have been collected. Second, the attenuation models for large earthquakes are not valid for the prediction of ground motion for low-to-moderate earthquakes, which can produce ground-motion levels that are of engineering interest (Campbell 1985; Frisenda et al. 2005).

In the present study, we present a technique for rapid computation of ground-shaking maps after moderate-to-large earthquakes (GRSmap). It takes advantage of the high density of the ISNet seismic stations and their wide dynamic ability to provide non-saturated, peak ground-motion measurements. The technique is based on an optimal data gridding scheme that uses triangulation, where the recording stations are the vertices of the triangles, thus obtaining a uniform coverage of the area of interest. The ground-motion measurements automatically provided by the EEWS are used for local correction of the predicted data at the barycentres of each triangle. The predictions are obtained by using the ad hoc attenuation relationship for the Campania-Lucania Region that was proposed by Convertito et al. (2007). Along with the other features of ISNet, the adopted gridding scheme and the local correction will allow the computation of maps that account for bi-dimensional earthquake features, such as radiation patterns, directivity and rupture extension, to which a great part of the damage are correlated.

To allow for site amplification effects in the predicted ground-shaking maps following the approach proposed by Park and Elrick (1998), a geological macro-zoning of the southern Apennines region was performed. The main geological units have been grouped based on age similarity, following the Quaternary-Volcanic-Tertiary-Mesozoic (QVTM) classification. A site-specific coefficient has been introduced for each class, to be used for correcting the estimates of peak ground-motion quantities at rock sites.

This technique proposed in the present study has been applied to the computation of ground-shaking maps for two earthquakes: a simulated  $M$  6.6 earthquake recorded at the ISNet seismic network and the 23 November 1980 Irpina  $M$  6.9 earthquake, the strongest earthquake that has occurred in the area to date.

## 2 The Irpinia Seismic Network: general overview

ISNet covers an area of approximately  $100 \text{ km} \times 70 \text{ km}$  along the southern Apennine chain, and it has been deployed to monitor the active fault system that generated the 1980 Irpinia earthquake. The ISNet configuration comprises an extended star topology that is designed to ensure fast and robust data recording, transmission and analysis. The configuration is based on four fundamental network elements: the seismic stations, the local control centres (LCCs), the central network control centre (RISSC), and the data communication systems (Weber et al. 2007). Figure 1 illustrates the locations of the stations of ISNet (squares); these are located along two concentric ellipses, with the major axes oriented NW–SE and parallel to the Apennine chain. The inter-station distances vary from ca. 10 km in the inner ellipse to ca. 20 km in the outer ellipse.

ISNet has 29 seismic stations that are grouped into six sub-nets that are each composed of a maximum of six or seven stations. The six LCCs (Fig. 1, grey circles) collect and store the data gathered by the seismic stations of the sub-net to which they are connected via digital radio. All LCCs use the Earthworm system for data collection and processing (Johnson et al. 1995).

To ensure a high dynamic range and to avoid signal saturation, each station is equipped with both three-component, strong-motion accelerometers and velocity instruments. In particular, all sites are equipped with a Guralp CMG5-T accelerometer and a short period ( $T_0 = 1 \text{ s}$ ) Geotech S13-Js sensor or a broad-band Nanometrics Trillium (0.025–50 Hz band) sensor (Weber et al. 2007). The data acquisition at the seismic stations is performed by a 24-bit, six channels data-logger: the Osiris-6 model (produced by Agecodagis) that includes Linux and open source software. The data are stored locally on a microdrive and continuously transmitted by Wi-Fi radio link to the nearest LCC.

At present, ISNet uses several different transmission systems. In particular, the seismic stations are connected via spread-spectrum radio links to the LCCs (Fig. 1, continuous line), and each LCC is connected through different technology and media types to the RISSC in Naples. The LCCs run the Earthworm real-time seismic-processing system and keep a complete local database of the waveforms from the seismic stations directly connected to them. The system will perform real-time event detection and location based on the triggers coming from data-loggers, along with parametric information, such as arrival-time picks coming from the other LCCs.

The ISNet data and information flow can be managed on three different levels: the recording sites, the LCCs and the RISSC in Naples. At the RISSC in Naples, the ISNet Devices Manager (ISNM) (<http://lxserver.ov.ingv.it>) has been developed for complete real-time monitoring and notification, which is aimed at reporting possible failures or the critical status of any of the network elements. A detailed description of the ISNet seismic network has been reported previously (Weber et al. 2007).

## 3 Methodology for ground-motion prediction in the southern Apennines

Ground-shaking maps are calculated by integrating data recorded by a seismic network with theoretical data, to achieve uniform cover of the area of interest. Theoretical data are obtained using empirical ground-motion relationships that for given magnitude and distance values allow the estimation of ground-motion parameters in both the time and frequency domains.

Aside from some empirical extensions to focal mechanisms (e.g. Abrahamson and Silva 1997; Boore et al. 1997), directivity effects (e.g. Somerville et al. 1997) and fault geometry (e.g. Ohno et al. 1993), the attenuation relationships assume a point-like seismic source and

isotropic radiation. Moreover, due to the averaging effects of the statistical regression used to retrieve the best model, the attenuation relationships cannot accurately account for azimuthal variations of peak ground motion that are due to source and/or path effects (e.g. site amplification, multi-path phenomena). On the other hand, for risk management, the latter can be dominant in the near source region of a moderate-to-large earthquake and can cause the largest part of the damage. As a consequence, the aim of the ground-shaking mapping technique is to partially overcome these limitations by using the information provided by recorded data.

Another problem when retrieving new attenuation models or existing models have to be used concerns the non-completeness of seismic catalogues, particularly for models with a large number of parameters. Furthermore, the attenuation relationships retrieved from large earthquakes might be inadequate to predict ground motion relative to low magnitude earthquakes. As a consequence, several ground-motion models for small earthquakes that can generate ground-motion levels of engineering interest (Campbell 1985) have been developed (Frisenda et al. 2005; Wald et al. 1999a). Additionally, the models obtained in a given seismotectonic environment are frequently used in areas with different seismic characteristics, when it is advisable to use data collected in the same region of interest for the retrieval of ground-motion-prediction models.

### 3.1 Ad hoc regional attenuation relationship

To limit these effects for the Campania-Lucania Region, Convertito et al. (2007) developed an ad hoc regional ground-motion attenuation relationship for the prediction of PGA and PGV values for moderate-to-large earthquakes. This attenuation model has a classical analytical formulation, and its coefficients were retrieved from an integrated observed and synthetic strong-motion database that was obtained using the stochastic approach proposed by Boore (1983). The input parameters for the simulation technique, i.e. the average static stress-drop values and attenuation parameters (geometric and anelastic), were obtained through spectral analysis of waveforms from earthquakes recorded by the Istituto Nazionale di Geofisica e Vulcanologia (INGV) seismic network for a magnitude range  $M_d$  (1.5, 5.0) over the last 15 years. The selected prediction model has the following formulation:

$$\log_{10} \text{Pgx} = a + bM + c \log_{10} \sqrt{R^2 + h^2} \pm \sigma \quad (1)$$

where  $\text{Pgx}$  corresponds to both PGA in  $\text{m/s}^2$  and PGV in  $\text{m/s}$ ,  $M$  is the magnitude and  $R$  is the epicentral distance in km. The coefficients and the standard error ( $\sigma$ ) on  $\log_{10} \text{Pgx}$  are listed in the first two rows of Table 1. Due to the aim of the present study, the third and fourth rows of Table 1 also list the coefficients of the same attenuation relationships obtained without introducing the PGA and PGV values of the 23 November 1980 Irpinia earthquake into the dataset (Convertito et al. 2007). This will allow the testing of the ability of the proposed ground-shaking technique to reproduce the PGA and PGV distributions, which are a function of distance from both the source and the azimuth, with respect to the predictions obtained using the attenuation relationships.

## 4 Geological macrozonation of the southern Apennines

Local site amplification effects on ground-shaking maps are accounted for using empirical corrective coefficients, the values of which depend on soil lithology and the amplitude and frequency content of the input ground motion, as suggested by Wald et al. (1999a).

**Table 1** Regression coefficients and standard errors of the regional attenuation relationship used to compute the ground-shaking maps (Convertito et al. 2007)

Pgx	<i>a</i>	<i>b</i>	<i>c</i>	<i>h</i>	$\sigma$
Pga (m/s <sup>2</sup> )	-0.559	0.383	-1.4	5.5	0.155
Pgv (m/s)	-3.13	0.570	-1.4	5.0	0.185
Pga (m/s <sup>2</sup> )*	-0.514	0.347	-1.4	5.5	0.145
Pgv (m/s)*	-3.04	0.552	-1.4	5.0	0.154

\* Indicate the coefficients of the same attenuation relationships obtained without introducing the PGA and PGV values of the 23 November 1980 Irpinia earthquake into the dataset

**Table 2** Site class definitions for the Campania-Lucania region and the corresponding EC8 site classes (2003)

Ground type	Age	Vs30 (m/s)	EC8 class
Carbonate platform successions	Mesozoic	>800	A
Sediments, soft rocks and Flysh deposit	Tertiary	360–800	B
Volcanic rocks	Tertiary–Quaternary	360–1000	B
Alluvium and gravel deposits	Quaternary	180–360	C
Very soft soils	Quaternary	<180	D

The amplification effects of near-surface geological layers critically depend on the shear-wave velocity and the thickness of the layers (e.g. Borchardt 1970; Joyner and Fumal 1985; Borchardt 1994). Following the approach proposed by Park and Elrick (1998), a site-map classification was first built for the southern Apennines region, and then an amplification coefficient was attributed to each class. The value of the coefficient depended on the soil class and the period of the input ground motion.

The site-map classification was obtained by grouping the main geological units present in the area into four macro-classes described by units with similar ages. The macro-classes considered were representative of alluvium (Quaternary), volcanic rock (Tertiary–Quaternary), soft rock (Tertiary) and hard rock (Mesozoic). The previous four classes have been overlapped on the 1:250,000 scale regional map, tracing only the geologic contacts separating units belonging to different categories. Then, based on a set of geotechnical soundings, borehole measurements and surface geology, a range of shear-wave velocities for the near-surface layer (Vs30) were assigned to each defined class. Table 2 lists the Vs30, associated to each of the geological units, classified following the main indications proposed by Eurocode 8 (2003) (EC8) (Cantore 2008). The map reporting this classification for the southern Apennines is indicated as a ‘QVTM’ map, which follows the notation used for a similar map proposed by Park and Elrick (1998) (Fig. 2).

For the corrective coefficients for the PGA and PGV estimates at a rock site, we used those reported by Wald et al. (1999a), except for the volcanic lithology, for which a preliminary value of 1.25 has been assumed, based on geological information (Cantore et al. 2008, unpublished data).

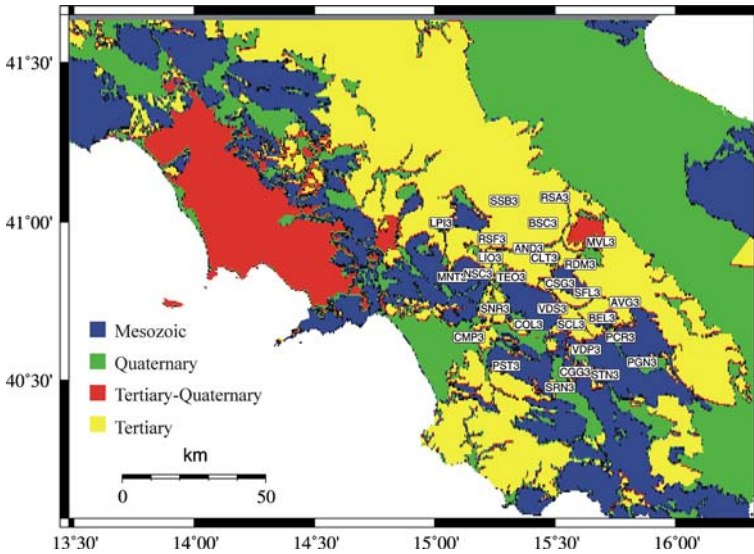


**Fig. 2** The QVTM site geological classification map. The legend reports the correspondence between colours and age. The labels indicate the locations of the ISNet seismic stations

## 5 Methodology outline for computation of the ground-shaking maps

Generally, ground-shaking maps are computed by interpolation of peak ground motions recorded at the seismic stations with predicted values estimated at selected points (phantom stations) chosen in an area not covered by the seismic network. The predicted ground-motion parameters, such as PGA and PGV, are usually estimated using empirical attenuation relationships. As a consequence, the predicted strong-motion field has a radial distribution, while due to the fault extension, focal mechanisms, and directivity effects, for example, the real field has a bi-dimensional distribution that depends upon both source-to-site distance and azimuth. This problem is faced in a different way by the existing techniques. For example, ShakeMap<sup>®</sup> allows fault extension to be accounted for by measuring the source-to-site distance to the surface fault projection, rather than to the epicentre.

The technique proposed in the present study, named GRsmap, is designed to work by taking advantage of the main characteristics of the ISNet seismic network. In particular, the study area is divided into data domains, referred to as the area covered by the seismic network and the external area. Different techniques are used in the two defined areas, both to define the location of the phantom stations and to correct the estimated ground-motion values. In the data domain, a triangulation scheme will allow to provide a more uniform distribution of stations covering the area of interest, while in the external area, a uniform grid of phantom stations was used.

The key aspects of this proposed methodology are the local nature of the estimate corrections, which are aimed at preserving the azimuthal properties of the recorded peak ground-motion field, and the automatic choice of the parameters controlling the distribution of the phantom stations.

The outline of the methodology can be schematically summarized as follows.

### 5.1 Triangulation of the data domain

- The recorded values of the peak amplitude are reduced to rock-site conditions by using the QVTM classification and the related correcting coefficients, as specified above.
- The seismic stations are the vertices of the triangles. For each triangle, the barycentre is identified and used as the phantom seismic station.
- The maximum acceptable area of each triangle cannot exceed  $N_A \times A_{ave}$ , where  $N_A$  is an integer that depends on the seismic network configuration, and  $A_{ave}$  is the average area of all the triangles. When a given area exceeds the fixed threshold, its barycentre will not be corrected, but the corresponding triangle will be recursively triangulated using the new barycentres as additional vertices. When the area is lower than the selected threshold value, at all the new barycentres the peak ground-motion parameters will be assigned using the estimates performed by the attenuation relationships corrected by the average residual calculated on a fixed number of real seismic stations.
- The epicentre is considered as an additional station. The datum at the epicentre is the estimated value at  $R = 0$  km using the attenuation relationship. This estimation is then corrected by an average residual, as explained below, computed at a number of stations surrounding the epicentre below a distance value that depends on seismic network density.
- For an earthquake located outside the data domain area, triangulation of the epicentral area is made denser and denser until a uniform station distribution is obtained.

### 5.2 Residual estimation

- When the optimal triangulation is achieved, the residuals are calculated at each vertex of the triangles by comparing the observed and the predicted ground-motion values obtained using Eq. 1. The average residual is then used to correct the predicted value at each barycentre. Formally, the general formulation of the attenuation relationships can be approximated as:

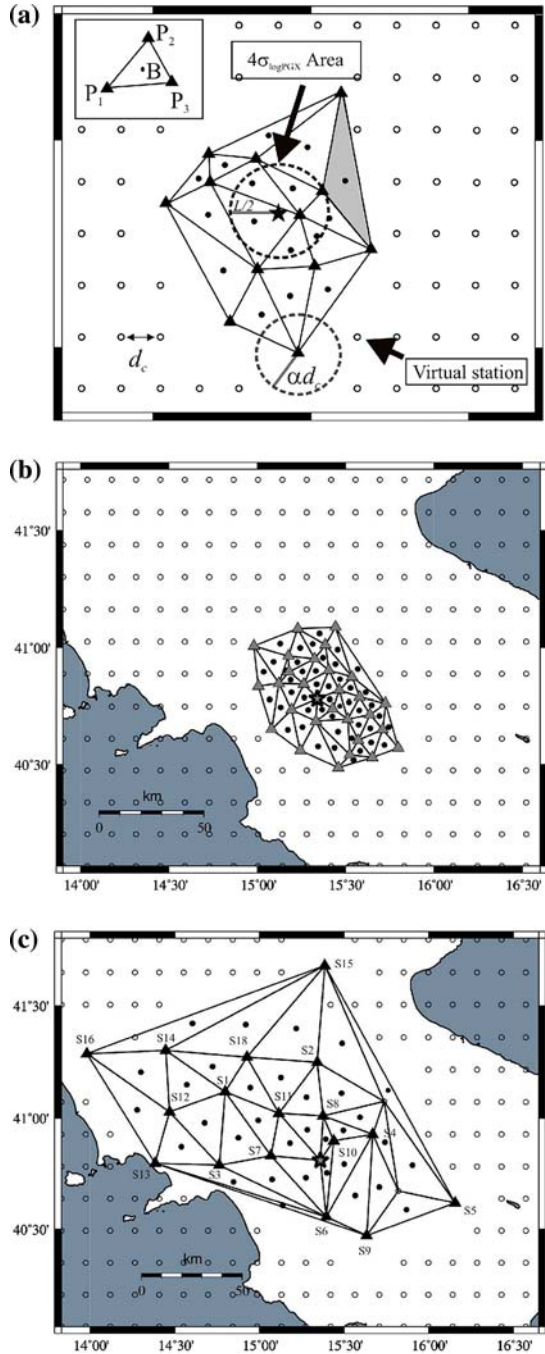
$$\log \text{Pgx}(R, \phi) = \log \text{Pgx}(R) + g(\phi) \tag{2}$$

where  $\text{Pgx}$  corresponds to either PGA or PGV,  $\log \text{Pgx}(R)$  is the standard distance–magnitude-dependent function, as Eq. 1, and  $g(\phi)$  is a term that accounts for azimuthal dependence of the peak ground motion. The correction scheme is aimed at estimating the term  $g(\phi)$ . Given the earthquake location and magnitude, the attenuation relationship (1) is used to obtain theoretical estimates at the network recording sites (Fig. 3, inset). Considering the  $i$ -th triangle, the vertices of which are labelled as  $P_1$ ,  $P_2$  and  $P_3$ , the peak motion residual term at the  $j$ -th vertex is computed as:

$$\text{Res}(P_j) = \log \text{Pgx}_j^{\text{obs}} - \log \text{Pgx}_j^{\text{est}} \tag{3}$$

where  $\text{Pgx}^{\text{obs}}$  is the recorded value and  $\text{Pgx}^{\text{est}}$  is estimated using the attenuation relationship (Eq. 1). The maximum acceptable residual value depends on the location of the vertices with respect to the epicentre. Based on the estimated fault length ( $L$ ), obtained using the Wells and Coppersmith (1994) relationships, an epicentral area is defined by a

**Fig. 3** **a** The main parameters of the triangulation scheme. *Black triangles* represent seismic stations, *black circles* the barycentres and *open circles* the virtual stations (phantom stations). **b** The triangulation for ISNet. **c** The triangulation for the network at which the 1980 Irpinia earthquake ( $M$  6.9) was recorded



circle of radius  $L/2$  centred on the epicentre. The residuals cannot exceed  $N\sigma_{\log P_{gx}}$ , where  $\sigma_{\log P_{gx}}$  is the standard error of Eq. 1 (Fig. 3a). The default value of  $N$  is generally fixed at 4 for sites located inside the epicentral area, otherwise 3. This choice is driven by the

hypothesis of log-normally distributed peak ground-motion values (Reiter 1990), and that at larger epicentral distances the attenuation relationships provide more reliable predictions. If a single residual is outside the fixed range, the datum is considered as an outlier and is not used in the map computation. This is because, a high residual value can indicate a possible station malfunctioning or strong site effect. In the first case, the datum has not been used while in the second case, the anomalous peak value cannot be properly corrected by the amplification coefficients which are an average measure of site amplification. Those data need specific analyses and can be thus introduced in a reviewed map but not in the version produced automatically. Otherwise, for a given triangle, the average peak motion residual term  $\langle \text{Res} \rangle_i$  is then obtained by:

$$\langle \text{Res} \rangle_i = \frac{1}{3} \sum_{j=1}^3 \text{Res}(P_j) \tag{4}$$

The quantity (4) is used to estimate the peak motion amplitude at the  $i$ -th barycentre point  $B_i$  according to

$$\log \text{Pgx}(B_i) = \log \text{Pgx}^{\text{est}}(B_i) + \langle \text{Res} \rangle_i \tag{5}$$

Equation 5 represents the estimated value of the ground-motion parameter corrected locally for azimuthal variations due to source effects, like directivity and focal mechanisms.

### 5.3 Extrapolation of peak motion in the external area

For the prediction of peak ground motion in the regions not covered by the seismic network, the main problem is the definition of the optimal grid spacing of the phantom stations and the threshold distance to the closest station where recorded data are available. This distance gives an empirical measure of the extent to which the observed data can be extrapolated outside the data domain area. In the proposed technique, the external area is covered with a uniform grid of phantom stations, the spacing interval of which is fixed to a fraction of the average distance between the stations and barycentres. The same value is used for the threshold distance (Fig. 3a).

Among all the nodes of the grid, only those located at distances larger than the threshold value from the closest recording station are retained for the extrapolation (Fig. 1, circles). At each retained node, the peak ground-motion parameter is then predicted using Eq. 1, adding a mean residual weighted for the epicentral distance, computed at seismic stations with an azimuth with respect to the epicentre, comparable with that of the considered phantom station. Estimated and recorded data are integrated and used to generate the ground-shaking map by re-interpolating onto a finer regular grid uniformly spaced at an arbitrary spacing interval of  $0.01^\circ$ . This map is finally corrected for site effects using the corrective coefficients corresponding to the site classification reported in Table 2.

## 6 Test and application

The technique proposed in the present study has been applied to two earthquakes: a simulated  $M$  6.6 seismic event with numerical accelerograms computed at the ISNet stations and the 23 November 1980 Irpinia earthquake ( $M$  6.9) recorded at a local seismic network. The use of a simulated earthquake is based on the necessity of testing the

procedure proposed in the present study on a large earthquake recorded at ISNet, while the choice of the Irpinia earthquake was driven by the fact that it is the strongest earthquake that has occurred in the area of interest.

For both of the earthquakes, ground-shaking maps in terms of PGA, PGV and instrumental intensity were calculated. We used the attenuation relationship proposed by Convertito et al. (2007), while the instrumental intensity was calculated by using the weighted average scheme and relationships proposed by Wald et al. (1999a), to convert PGA and PGV into instrumental intensity. On the other hand, for future applications, the use of a more robust strong ground-motion attenuation relationships and of relationships to convert strong ground-motion parameters into macroseismic intensities retrieved from an Italian database, such as that proposed by Faccioli and Cauzzi (2006), would be desirable.

### 6.1 The simulated $M$ 6.6 earthquake

The simulation technique proposed by Gallovič and Brokešhová (2007) was used to calculate the broad-band synthetic accelerograms at each site of ISNet. The rupture process at the seismic source was described in terms of the slipping of elementary sub-sources of various sizes, randomly distributed on the fault plane. At low frequencies, the source was described by the representation theorem (Aki and Richards 1980), assuming a  $k$ -squared distribution (Herrero and Bernard 1994; Gallovič and Brokešhová 2004) for the final slip (integral approach). At high frequency, the ground-motion synthesis was obtained by summing the contributions from each individual sub-source (composite approach). In other words, at large scales, the faulting process is completely equivalent to the classical  $k$ -squared model, while at low scales, the sub-source behaviour becomes chaotic and the radiated wave-field appears to be isotropic. The synthetic seismograms computed using both the integral and the composite approaches were then combined in the frequency crossover range by a weighted average of both real and imaginary parts of the respective Fourier spectra. Finally, to allow for the propagation effects, an evaluation of the Green functions was required. For a one-dimensional propagation medium, the source model was combined with the discrete wave-number technique by Bouchon (1981) so as to obtain full wave-field Green functions.

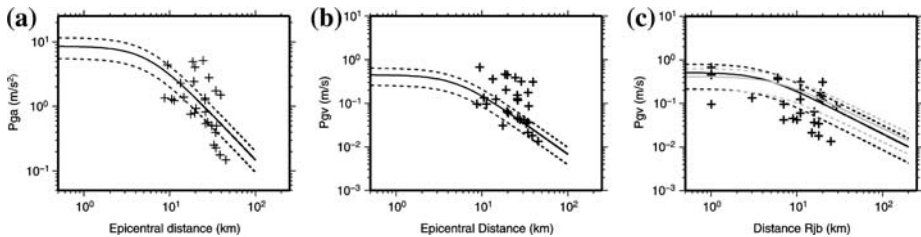
The parameters selected for the simulation are listed in Table 3. Notice that these parameters correspond to those characterizing the main fault of the 23 November 1980 Irpinia earthquake (Table 4,  $F_1$ ). The peak ground-motion parameters (PGA and PGV) measured on the synthetic waveforms are used as input data for the computation of the ground-shaking map. The comparison with the estimated values obtained by the attenuation relationships proposed by Convertito et al. (2007) is reported in panels a and b of

**Table 3** Fault parameters of the  $M$  6.6 simulated earthquake

Parameter	Value
Length (km)	35
Width (km)	15
Depth of the top (km)	2.2
Strike (°)	315
Dip (°)	60
Slip (°)	−90
Seismic moment (Nm)	$1.3 \times 10^{19}$

**Table 4** Fault parameters of the 23 November 1980 Irpinia earthquake (after Bernard and Zollo 1989)

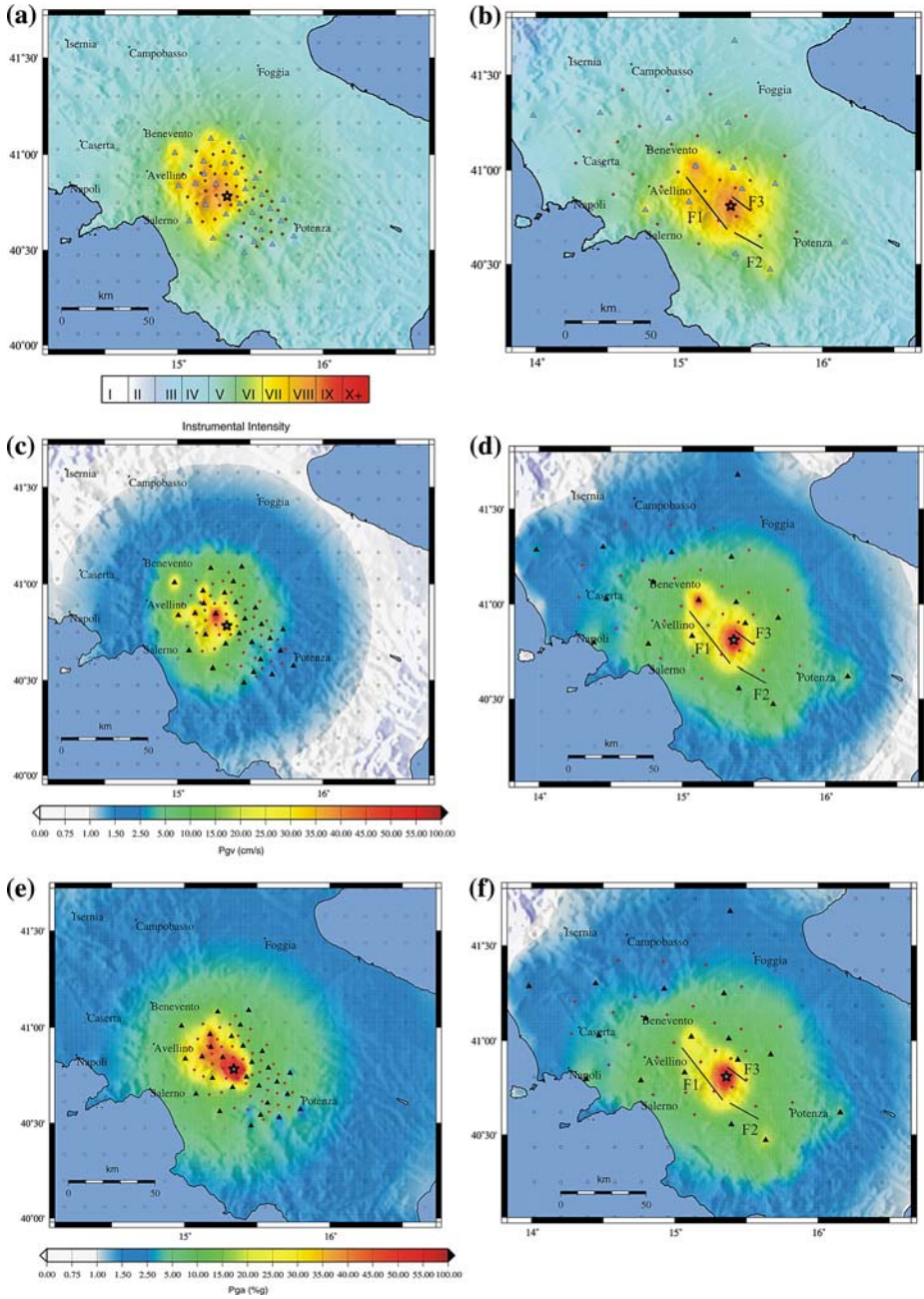
Parameter	F <sub>1</sub>	F <sub>2</sub>	F <sub>3</sub>
Length (km)	35	20	20
Width (km)	15	15	10
Depth of the top (km)	2.2	10	2.2
Strike (°)	315	300	124
Dip (°)	60	20	70
Slip (°)	−90	−90	−90
Seismic moment (Nm)	$2 \times 10^{19}$	$4 \times 10^{18}$	$3 \times 10^{18}$



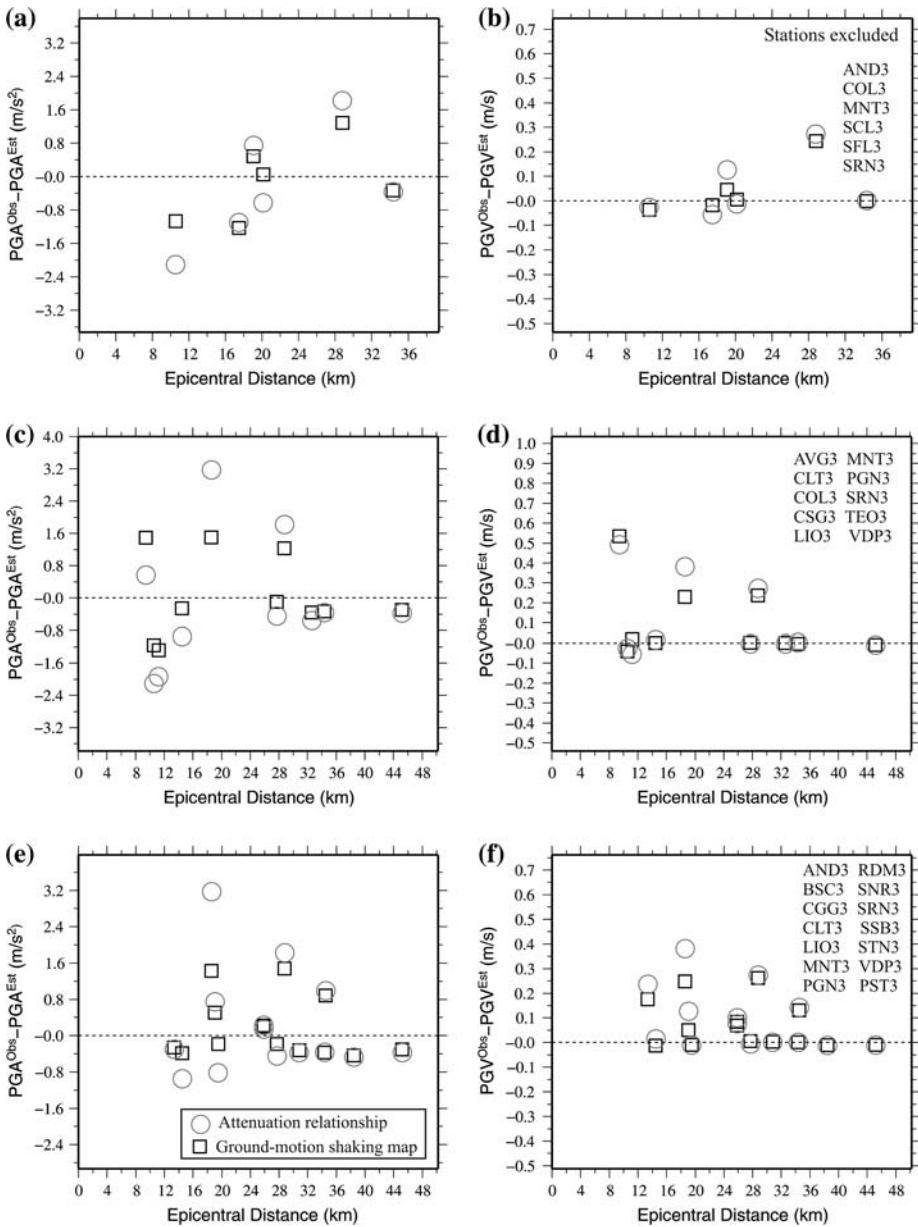
**Fig. 4** Validation of synthetic PGA (a) and PGV (b) values. On each panel, the crosses represent the PGA and PGV values retrieved from the synthetic waveforms simulated at the ISNet recording stations. Black lines on panels a and b refer to the median values of the Convertito et al. (2007) attenuation relationships, while dashed lines refer to  $\pm 1\sigma$ . Panel c shows the same data when the minimum fault distance (Rjb) is taken into account. Black lines refer to Sabetta and Pugliese (1996) attenuation relationship, while grey lines refer to Akkar and Bommer (2007) attenuation relationship

Fig. 4. In particular, the continuous lines correspond to the median values, the dashed lines to  $\pm 1\sigma$  and the crosses to the simulated data. Notice that the PGA data are in good agreement with the adopted attenuation relationship, while there are some discrepancies for PGV that can be attributed primarily to the directivity effect and to the distance definition that, for large earthquakes, should be the fault distance rather than the epicentral distance. In fact, when the minimum fault distance (Rjb) is used, the data distribution is in agreement with classical attenuation relationships. As an example, panel c of Fig. 4 shows the comparison between the data plotted as a function of the Rjb distance (crosses) and two attenuation relationships, which account for the Rjb distance. In particular, black lines refer to the attenuation relationship proposed by Sabetta and Pugliese (1996) while grey lines refer to the attenuation relationship proposed by Akkar and Bommer (2007). For both the attenuation relationships, the dashed lines refer to  $\pm 1\sigma$ .

According to the methodology explained in the previous paragraph, the triangulation scheme and the distribution of the phantom and ISNet stations are reported in Fig. 3b. The average area of the triangles is about 67 km<sup>2</sup>, while the threshold distance and phantom spacing grid is 30 km. Figure 5a, c, e shows the maps for PGA as percentage of gravity acceleration (g), PGV in cm/s and instrumental intensity calculated using the technique proposed in the present study. At large distances from the epicentre (>50 km), the maps show a radial symmetry, while in the epicentral area, a distribution elongated in the N–W direction is evident. This elongation can be interpreted as being due to the fault extension and the directivity effect towards the north-west.



**Fig. 5** Ground-shaking maps of PGA, PGV and instrumental intensity for the simulated  $M 6.6$  earthquake (a, c, e) and for the 23 November 1980  $M 6.9$  Irpinia earthquake (b, d, f). The triangles represent the seismic stations, the circles the phantom stations and the red points the barycentres. b, d, f The black lines represent the three fault segments (F<sub>1</sub>, F<sub>2</sub> and F<sub>3</sub>) that ruptured during the Irpinia earthquake



**Fig. 6** Residuals analysis for synthetic PGA (a, c, e) and PGV (b, d, f) values. *Black squares* refer to data extracted from ground-shaking maps, while *grey circles* refer to the PGA and PGV values obtained using the attenuation relationships. The list of excluded stations is reported in the upper right corner

To validate the ground-shaking map technique, additional tests have been performed while excluding an increasing number of stations (6, 10 and 14 stations) from the input dataset. Next, given the new maps, the PGA and PGV data at points corresponding to the excluded stations were extrapolated from the maps and compared with the original input

data. Figure 6 shows the results of the test in terms of residuals between observed and estimated PGA and PGV data. In particular, the squares correspond to the residuals when the estimated data are retrieved from the maps using the interpolation procedure, while the grey circles correspond to the residuals obtained when the attenuation relationships are used to estimate the PGA and PGV values. The ground-shaking maps provide estimates with a lesser residual with respect to the attenuation relationship. The values of the residuals depend on the epicentral distance and, in particular, on the azimuth of the excluded station. The difference between the two residuals decreases with increasing number of excluded stations, as a consequence of the fact that when a larger number of stations are excluded the estimates have a larger weight with respect to the observations. Furthermore, the results in Fig. 6 show that the residuals on PGV are almost all positive. This result reflects the discrepancy between predicted and simulated PGV values for stations affected by source effect, such as focal mechanism and directivity effect which are more evident at low frequency (Fig. 4b).

## 6.2 The 23 November 1980 Irpinia earthquake ( $M$ 6.9)

The 23 November 1980 Irpinia earthquake ( $M$  6.9) is one of the largest destructive earthquakes that has occurred in Italy over the last century. It was characterized by a complex normal faulting that ruptured three different sub-parallel fault segments of the southern Apennine belt chain (Westaway and Jackson 1984; Bernard and Zollo 1989; Pantosti and Valensise 1990). The parameters of the three faults are listed in Table 4. The strong-motion records from a local seismic network managed by ENEA–ENEL were available to compute the ground-shaking maps. The 18 seismic stations were equipped with SMA-1 accelerographs (Berardi et al. 1981). Figure 3c shows the location of the seismic stations (triangles) and instrumental epicentre (grey star). The phantom stations (circles), the triangulation scheme and the barycentres (black dots) are also shown in Fig. 3c. The average area of the triangles is about  $473 \text{ km}^2$ , while the threshold distance and phantom spacing of the grid is 62 km.

To highlight the advantages of the technique proposed in the present study, the ground-shaking maps were calculated using the attenuation relationships retrieved from the dataset that did not include data from the Irpinia earthquake considered. Figure 7 shows the PGA and PGV values (crosses) recorded during the Irpinia earthquake, compared with the attenuation relationships (black and grey lines). Note that when the PGA corresponding to the Irpinia earthquake was used to retrieve the attenuation relationships (black lines), the fit was improved and the median value was more reliable. On the other hand, the underestimations in PGV are mainly attributed to the initial attenuation model, i.e. the attenuation relationship proposed by Convertito et al. (2007). In order to show how the corrective scheme allows to recover the discrepancies between observed and predicted data, in Fig. 7 are also shown the attenuation relationships obtained by using data retrieved from the final ground-shaking maps shown in Fig. 5. In particular, black dots and error bars shown in both panels a and b of Fig. 7 are retrieved from the ground-shaking maps along four different profiles centred in the earthquake's epicentre (star in Fig. 5) and oriented at azimuths:  $0^\circ$ ,  $45^\circ$ ,  $90^\circ$  and  $135^\circ$ . The data were averaged and standard errors were computed by using a 10-km binning on the epicentral distance. The red lines on both panels represent the best data fitting while the dashed lines refer to  $\pm 1\sigma$ . It can be noted how the final maps account for the initial discrepancies with respect to the initial adopted attenuation relationships.

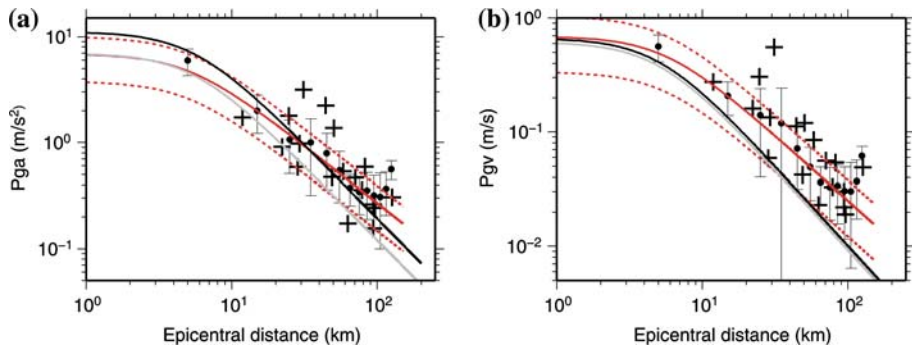


**Fig. 7** PGA (a) and PGV (b) values (*crosses*) recorded during the 23 November 1980  $M$  6.9 Irpinia earthquake. *Grey lines* refer to the attenuation relationships proposed by Convertito et al. (2007), when the PGA and PGV values of the Irpinia earthquake are not included in the dataset, while *black lines* refer to the same attenuation relationships obtained when they are included in the dataset. On each panel, *black dots* and *error bars* refer to PGA and PGV values extracted from the final ground-shaking maps; *continuous red lines* refer to the best fitting while *red dashed lines* refer to  $\pm 1\sigma$

The computed ground-shaking maps are shown in Fig. 5b, d, f. In particular, Fig. 5b shows the map of instrumental intensity; Fig. 5d shows the PGV map expressed in cm/s; and Fig. 5f shows the PGA maps expressed as percentages of gravity acceleration. In each panel of Fig. 5, the triangles correspond to the seismic stations, the star corresponds to the instrumental epicentre, the three black lines indicated as  $F_1$ ,  $F_2$  and  $F_3$  correspond to the three fault segments that ruptured during the earthquake, and the dots with the crosses correspond to the barycentres of the triangles.

The main features of the complex fault mechanism characterizing the 1980 Irpinia earthquake are highlighted on the maps. Although the predictive attenuation model was based on the assumption of a point-like source, the maps reproduce the extension of the three fault segments and the associated complex ground-motion pattern. This can be attributed to the use of recorded data and corrected estimates at the barycentres that provide improved coverage of the source area. Both the PGA and PGV maps reproduce the directivity effect, which is towards the north-west for fault segment  $F_1$  and towards the south-east for fault segment  $F_2$ , and it is identifiable by the larger ground-motion values in those directions. Moreover, due to the technique adopted to compute instrumental intensity, which used a weighted average scheme between the two relationships proposed by Wald et al. (1999b) to convert PGA and PGV into instrumental intensities, the corresponding intensity maps for both the selected earthquakes are directly connected to the PGA and PGV maps.

## 7 Conclusion

In the present study, we have presented a technique for ground-shaking map computation. This technique, named GRSmap, works by taking advantage of the characteristics of the ISNet installed in the Campania-Lucania Region, and it was designed as a tool for directing first-aid emergency rescue by the Regional Civil Protection.

The technique uses two different approaches to cover the data domain: area covered by the seismic network and external area. In particular, the interpolation in the data domain is

performed by using a triangulation scheme between the stations, and adding as further data the estimates at the barycentres using an ad hoc attenuation relationship, corrected to account for the characteristics of the selected earthquake.

The triangulation scheme allows for local correction that accounts for the azimuthal characteristics of the strong-motion field that are generally not accounted for the classical attenuation relationships. Additionally, the correction is based on the azimuth and distance of each barycentre from the epicentre and on the comparison of this distance with the empirical fault length estimated using the Wells and Coppersmith (1994) relationships.

We have tested the proposed technique first on a simulated  $M$  6.6 earthquake at the ISNet seismic stations and then applied it to the data from the 23 November 1980 Irpinia ( $M$  6.9) earthquake. This has highlighted the ability of this proposed method to produce ground-shaking maps containing bi-dimensional source effects, such as directivity or focal mechanism, with respect to the estimates performed using classical attenuation relationships. Furthermore, the ground-shaking maps relative to the Irpinia earthquake reproduce quite well the features of the complex fault mechanism that characterized this event, although the data was recorded at a sparse seismic network.

**Acknowledgement** The authors wish to thank František Gallovič for providing the simulations, two anonymous reviewers and an anonymous referee for their thorough reviews and helpful comments. The figures were prepared using GMT software (Wessel and Smith 1991). This work was financially supported by AMRA scarl ([www.amra.unina.it](http://www.amra.unina.it)) in the frame of the SAFER project (sixth framework programme sustainable development, global change and ecosystem priority 6.3.IV.2.1: reduction of seismic risks contract for specific targeted research or innovation project contract no. 036935) and in collaboration with the Italian Dipartimento della Protezione Civile in the frame of the SAMS project.

## References

- Abrahamson NA, Silva WJ (1997) Empirical response spectral attenuation relations for shallow crustal earthquakes. *Seismol Res Lett* 68:94–127
- Aki K, Richards PG (1980) *Quantitative seismology: theory and methods*, vols 1 and 2. W. H. Freeman and Co., San Francisco, 932 pp
- Akkar S, Bommer JJ (2007) Empirical prediction equations for peak ground velocity derived from strong-motion records from Europe and the Middle East. *Bull Seismol Soc Am* 97:511–530. doi: [10.1785/0120060141](https://doi.org/10.1785/0120060141)
- Allen R (2007) The ElarmS earthquake early warning methodology and application across California. In: Gasparini P (ed) *Earthquake early warning systems*. Springer, Berlin, pp 133–152
- Berardi R, Berenzi A, Capozza F (1981) Campania-Lucania earthquake on 23 November 1980: accelerometric recordings of the main quake and relating processing. Technical report, Ente Nazionale per l'Energia Elettrica (ENEL), Rome
- Bernard P, Zollo A (1989) The Irpinia (Italy) 1980 earthquake: detailed analysis of a complex normal fault. *J Geophys Res* 94:1631–1648
- Boore DM (1983) Stochastic simulation of high-frequency ground motion based on seismological models of the radiated spectra. *Bull Seismol Soc Am* 73:1865–1893
- Boore DM, Joyner WB, Fumal TE (1997) Equations for estimating horizontal response spectra and peak acceleration from western North American earthquakes: a summary of recent work. *Seismol Res Lett* 68:128–153
- Borcherdt RD (1970) Effects of local geology on ground motion near San Francisco Bay. *Bull Seismol Soc Am* 60:29–61
- Borcherdt RD (1994) Estimates of site-dependent response spectra for design (methodology and justification). *Earthq Spectra* 10:617–654
- Bouchon M (1981) A simple method to calculate Green's functions for elastic layered media. *Bull Seismol Soc Am* 74:1615–1621
- Campbell KW (1985) Strong motion attenuation relations: a ten-year perspective. *Earthq Spectra* 1:759–804

- Cantore L (2008) Determination of site amplification in the Campania-Lucania region (southern Italy) by comparison of different site-response estimation techniques. Ph.D. thesis, Dip. di Fisica, Università Federico II di Napoli
- Cantore L, Convertito V, Zollo A, Elia L (2008) Site-condition map and site amplification corrections for early-warning applications and seismic hazard assessment in the Campania-Lucania Region (southern Apennines), Italy (in preparation)
- Cinti FR, Faenza L, Marzocchi W, Montone P (2004) Probability map of the next  $M \geq 5.5$  earthquakes in Italy. *Geochem Geophys Geosyst* 5:Q1103. doi:10.1029/2004GC000724
- Convertito V, De Matteis R, Romeo A, Zollo A, Iannaccone G (2007) Strong motion relation for early-warning applications in the Campania Region (southern Apennines), Italy. In: Gasparini et al (eds) *Earthquake early warning systems*. Springer-Verlag, Berlino
- Dreger D, Kaverina A (2000) Seismic remote sensing for the earthquake source process and near-source strong shaking: a case study of the October 16, 1999 Hector mine earthquake. *Geophys Res Lett* 27:1941–1944
- Eurocode 8 (2003) Design of structures for earthquake resistance. Part 1: general rules, seismic actions and rules for buildings. Draft January 2003
- Faccioli E, Cauzzi C (2006) Macroseismic intensities for seismic scenarios, estimated from instrumentally based correlations. In: 1st European conference on earthquake engineering and seismology, Geneva, 3–8 Sept 2006, Paper no. 569
- Frisenda M, Massa M, Spallarossa D, Ferretti G, Eva C (2005) Attenuation relationship for low magnitude earthquakes using standard seismometric records. *J Earthq Eng* 9:23–40
- Gallovič F, Brokešhová J (2004) On strong ground motion synthesis with  $k^{-2}$  slip distributions. *J Seismol* 8:211–224
- Gallovič F, Brokešhová J (2007) Hybrid  $k$ -squared source model for strong ground motion simulation: introduction. *Phys Earth Planet Inter* 160:34–50
- Goltz JD (2003) Applications for new real-time seismic information: the TriNet project in southern California. *Seismol Res Lett* 74:516–521
- Herrero A, Bernard P (1994) A kinematic self-similar rupture process for earthquakes. *Bull Seismol Soc Am* 84:1216–1228
- Jean WY, Chang YW, Wen KL, Loh CH (2006) Early estimation of seismic hazard for strong earthquakes in Taiwan. *Nat Hazards* 37:39–53
- Johnson CE, Bittenbinder A, Bogaert B, Dietz L, Kohler W (1995) Earthworm: a flexible approach to seismic network processing. *IRIS News* 14:1–4
- Joyner WB, Fumal TE (1985) Predictive mapping of earthquake ground motion. In: Ziony JE (ed) *Evaluating earthquake hazard in the Los Angeles region—an earth-science perspective*. U.S. Geological Survey professional paper 1360, pp 203–220
- Ohno S, Ohta T, Ikeura T, Takemura M (1993) Revision of the attenuation formula considering the effect of fault size to evaluate strong ground motion spectra in near field. *Tectonophysics* 218:69–81
- Pantosti D, Valensise G (1990) Faulting mechanism and complexity of the 23 November 1980, Campania-Lucania earthquake inferred from surface observations. *J Geophys Res* 134:15319–15341
- Park S, Elrick S (1998) Predictions of shear wave velocities in southern California using surface geology. *Bull Seismol Soc Am* 88:677–685
- Reiter L (1990) *Earthquake hazard analysis—issues and insights*. Columbia University Press, New York, 254 pp
- Sabetta F, Pugliese A (1996) Estimation of response spectra and simulation of nonstationary. *Bull Seismol Soc Am* 86:337–352
- Somerville PG, Smith HF, Graves RW, Abrahamson NA (1997) Modification of empirical strong ground motion attenuation relationship to include the amplitude and duration effects of rupture directivity. *Seismol Res Lett* 68:199–222
- Wald DJ, Quitoriano V, Heaton TH, Kanamori H, Scrivner CW, Worden CB (1999a) TriNet shakemaps: rapid generation of instrumental ground motion and intensity maps for earthquakes in southern California. *Earthq Spectra* 15:537–555
- Wald DJ, Quitoriano V, Heaton TH, Kanamori H (1999b) Relationship between peak ground acceleration, peak ground velocity, and modified Mercalli intensity for earthquakes in California. *Earthq Spectra* 15:557–564
- Weber E, Convertito V, Iannaccone G, Zollo A, Bobbio A, Cantore L, Corciulo M, Di Crosta M, Elia L, Martino C, Romeo A, Satriano C (2007) An advanced seismic network in southern Apennines (Italy) for seismicity investigations and experimentation with earthquake early warning. *Seismol Res Lett* 78:622–634

- Wells DL, Coppersmith KJ (1994) New empirical relationships among magnitude, rupture length, rupture width, rupture area, and surface displacement. *Bull Seismol Soc Am* 84:974–1002
- Wessel P, Smith WHF (1991) Free software helps map and display data. *EOS Trans Am Geophys Union* 72(441):445–446
- Westaway RWC, Jackson J (1984) Surface faulting in the southern Italian Campania-Basilicata earthquake of 23 November 1980. *Nature* 312:436–438